ON THE MULTI-CHANNEL ANDERSON IMPURITY MODEL OF URANIUM COMPOUNDS

N. ANDREI and C. J. BOLECH
Rutgers University

Abstract. In this talk we will present the solution of the two-channel Anderson impurity model, proposed in the context of the heavy fermion compound UBe_{13}, and discuss briefly the more general multi-channel case. We will show results for the thermodynamics in the full range of temperature and fields and make the connection with the current experimental situation.

1. Models of Uranium ions

During the last two decades, there has been growing interest in materials whose desciption falls outside the framework of Landau's Fermi Liquid Theory. Examples are the high T_c superconductors, heavy fermions and quasi-1D conductors.

Uranium heavy fermion compounds provide very interesting examples, exhibiting unusual specific heat temperature dependence, $\gamma = C_V/T \sim \ln T$. This behavior is often related to multichannel Kondo physics, occasioned in the case of Uranium by the ground state configuration which is degenerate and non-magnetic, so that one is lead to consider a quadrupolar Kondo scenario (1, 2).

The starting point is to consider the energies of the uranium ion in its different states of valence. They fall on a parabola depicted in Fig. 1. The ground state corresponds to a U^{4+} ionization state, with a $5f^2$ shell-configuration. Considering the spin-orbit Hund's coupling, the lowest multiplet corresponds to $J = 4$. Taking, further, into account the splitting due to a cubic crystal field (as is the case for the heavy fermion compound UBe_{13}) one finds that the lowest multiplet corresponds to a non-Kramers Γ_3 doublet (see Fig. 1).

A similar analysis for the neighboring states of valence indicates that they corresponds to: (**i**) U^{3+}: a $5f^3$ shell-configuration that splits giving a $J = 9/2$ lowest multiplet configuration, that further splits giving a lowest Γ_6 Kramer's doublet and (**ii**) U^{5+}: a $5f^1$ shell-configuration that splits giving

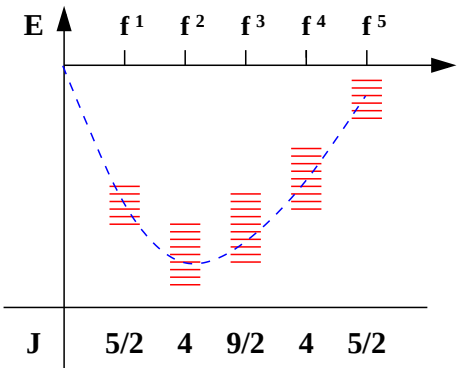

Figure 1. Schematics of the energy and lowest angular momentum multiplet for different states of valence of a uranium ion.

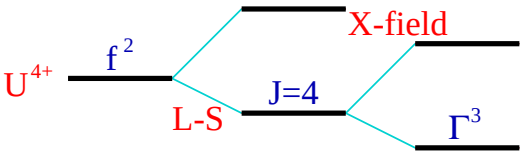

Figure 2. Schematic depiction of the spin-orbit and crystal field splittings for the ground state valence configuration of uranium in a cubic medium.

a $J = 5/2$ lowest multiplet configuration, that further splits giving a lowest Γ_7 Kramer's doublet. These three valence states are in fact very close in energy and their relative positions are not completely resolved, since the experimental evidence is not conclusive and sometimes contradictory (3, 4). The most accepted scenario is that of a Γ_3 quadrupolar doublet ground state coming from the tetravalent state and next a Γ_6 magnetic doublet coming from the trivalent state of uranium. Neglecting the contributions from the pentavalent state of the uranium as well as those from excited crystalline electric field states we can write down the following Hamiltonian, the *two-channel Anderson impurity model* (see Fig. 1 for a schematic depiction).

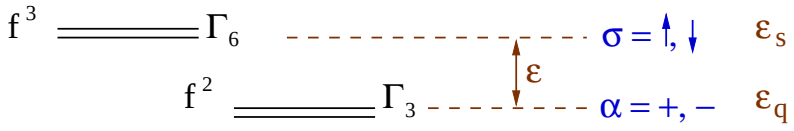

Figure 3. Schematics of the electronic configurations and symmetry multiplets retained for the Hamiltonian of UBe_{13}.

$$
\begin{aligned}
H_{\Gamma_3,\Gamma_6} = H_{\rm host} \; &+ \; \varepsilon_q \sum_{\alpha} b^\dagger_{\bar\alpha} b_{\bar\alpha} + \varepsilon_s \sum_{\sigma} f^\dagger_\sigma f_\sigma \\
&+ \; V \sum_{k,\alpha,\sigma} \left[f^\dagger_\sigma b_{\bar\alpha} c_{k,\alpha,\sigma} + c^\dagger_{k,\alpha,\sigma} b^\dagger_{\bar\alpha} f_\sigma \right] \\
\text{with} \qquad {\rm Q} \; &= \; \sum_{\alpha} b^\dagger_{\bar\alpha} b_{\bar\alpha} + \sum_{\sigma} f^\dagger_\sigma f_\sigma = 1
\end{aligned}
$$

where the bar on top of the index α indicates that it transforms according to the complex conjugate representation. We used *slave-boson* language and denoted $\varepsilon_q \equiv E_{\Gamma_3}$ and $\varepsilon_s \equiv E_{\Gamma_6}$ (let us also define $\varepsilon \equiv \varepsilon_s - \varepsilon_q$ and $\Delta \equiv V^2/2$). Notice that the model has full $SU(2) \otimes SU(2)$ internal symmetry. In the parameter regimes when $|\varepsilon| \gg \Delta$, we can map it via a Schrieffer-Wolff transformation into a quadrupolar two-channel Kondo model (with a localized quadrupolar moment in the case when $\varepsilon_q \ll \varepsilon_s$), or a magnetic two-channel Kondo model (with a localized magnetic moment in the case when $\varepsilon_q \gg \varepsilon_s$), in both cases with a coupling constant given by $J = V^2/|\varepsilon_s - \varepsilon_q|$ (assuming zero chemical potential).

We will also consider a generalized version of the Hamiltonian, the *multi-channel Anderson impurity model*. In *slave-boson* language the Hamiltonian looks exactly as in the two-channel case, but this time the indices take values according to: (**i**) $\sigma = 1, \ldots, N$ and (**ii**) $\alpha = 1, \ldots, M$. If we follow the standard nomenclature we would call σ the spin index and α the channel index, and the model will be the $SU(N) \otimes SU(M)$ version of the multi-channel Anderson model (5).

As in the two-channel case we can perform Schrieffer-Wolff transformations to derive effective models in any of the two local moment regimes of the problem. When $\varepsilon_q \ll \varepsilon_s$ (assuming always zero electronic chemical potential) we obtain an 'N-channel $SU(M)$ Coqblin-Schrieffer model', whereas when $\varepsilon_s \ll \varepsilon_q$ we obtain an 'M-channel $SU(N)$ Coqblin-Schrieffer model'.

This model has been extensively studied over the past fifteen years by a variety of methods: Large-N methods (6), NCA (4), conserving T-matrix approximation (7), Monte Carlo (4) and Numerical Renormalization Group (8) among others. All these techniques have difficulties accessing the mixed valence regime.

We showed that this model is integrable and carried out a full analysis by means of the Bethe Ansatz technique. That allowed us to obtain exact results characterizing the ground state of the model as a function of its parameters and very accurate numerical results for the thermodynamics of the model for all temperatures and fields, as well as all valence regimes, including the mixed valence. We stress that is in the mixed valence regime where

the Bethe Ansatz solution is most crucial, since all the other techniques have difficulties accessing it.

2. The Thermodynamics of the Model

In this section we present the results of the numerical solution of the Thermodynamic Bethe Ansatz equations for the two-channel case (i.e. $N = M = 2$). This is the first model proposed in the context of UBe_{13}(1). We will study the physics of the model on its own right and also briefly discuss its virtues and inadequacies to describe the physics of the uranium compound that motivated it. The conclusion that we will reach is that one needs to go beyond the simplest scenario given by the two-channel model.

In Fig. 2 we show the behavior of the impurity entropy as a function of temperature for different values of $(\varepsilon - \mu)$, and in Fig. 2 the reader can see the effect of switching on an external field.

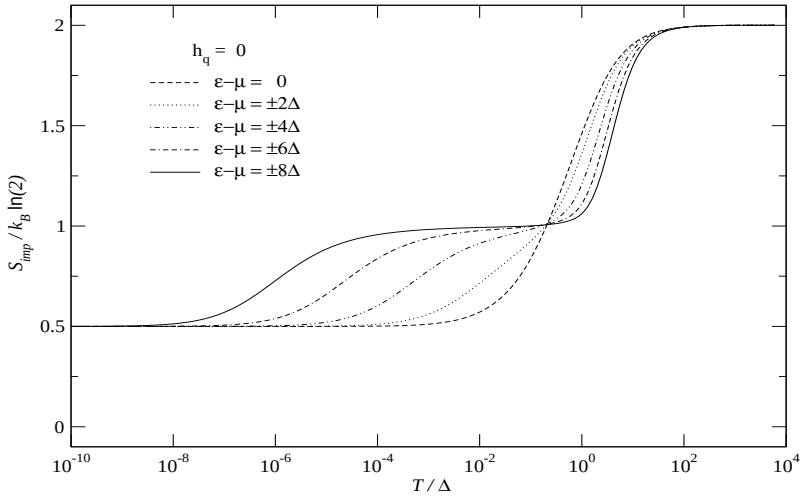

Figure 4. Impurity contribution to the entropy at zero field and as a function of temperature for different values of $\varepsilon - \mu$. As the temperature goes to zero all curves approach the universal value $k_B \ln\sqrt{2}$. Positive and negative values of $\varepsilon - \mu$ fall on top of each other.

At high temperatures the entropy is $S_{\rm imp} = k_{\rm B} \ln 4$ in agreement with the size of the impurity Hilbert space. For $|\varepsilon - \mu| \gg \Delta$ the impurity entropy is *quenched* in two stages. The degrees of freedom corresponding to the higher energy doublet are frozen first. The entropy becomes $S_{\rm imp} = k_{\rm B} \ln 2$ and the system is in a localized magnetic or quadrupolar moment regime depending on the sign of $(\varepsilon - \mu)$. As the temperature is further decreased,

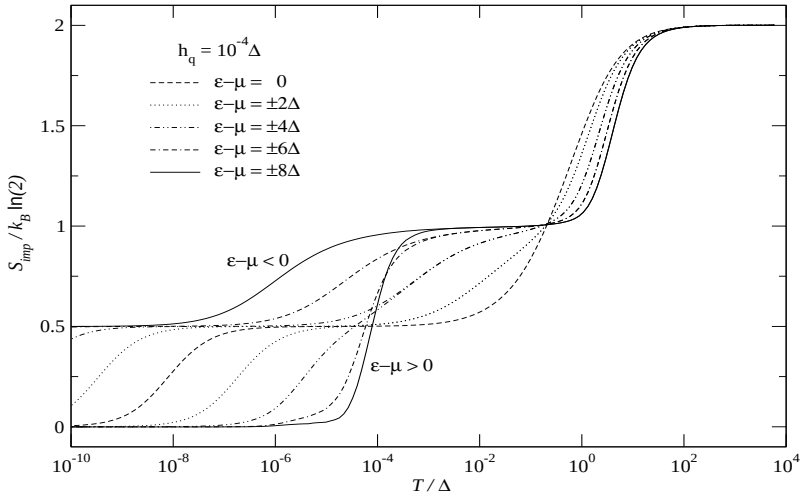

Figure 5. Impurity contribution to the entropy in the presence of an applied quadrupolar field and as a function of temperature for different values of $\varepsilon - \mu$. As the temperature goes to zero all curves approach zero. Positive and negative values of $\varepsilon - \mu$ fall on top of each other only at high temperatures and, asymptotically, for low temperatures.

the remaining degrees of freedom undergo frustrated screening leading to entropy $S_{\rm imp} = k_{\rm B} \ln \sqrt{2}$. On the other hand, for values of $|\varepsilon - \mu| \ll \Delta$, the quenching process takes place in a single stage. The initial stage of the quenching process happens when the system makes the transition from a high-energy state of valence $n_c = \frac{1}{2}$ (i.e. when both states of valence are equally likely) to the state of valence that will be present at low-energies, $n_c^0(\varepsilon - \mu)$. This is further illustrated in Fig. 2.

As $(\varepsilon - \mu)$ is varied, the behavior interpolates continuously between the magnetic ($n_c^0 = 1$) and the quadrupolar ($n_c^0 = 0$) scenarios. The zero temperature entropy is found to be independent of ε in accordance with our analytic results (9). External fields, either magnetic or quadrupolar, constitute relevant perturbations that drive the system to a Fermi Liquid fixed point with zero entropy.

In Fig. 2 we show the impurity contribution to the specific heat. The two stage quenching process gives rise to two distinct peaks. The lower temperature peak is the Kondo contribution centered around a temperature $T_l\,(\varepsilon - \mu)$, whereas the higher temperature peak – often referred to as the Schottky anomaly – is centered around a temperature $T_h\,(\varepsilon - \mu)$. Approximate expressions for $T_{h,l}$ can be read off from the curves:

$$T_{h,l}(\varepsilon) \approx \frac{\Delta}{a\pi^2} \ln(1 + 2a\, e^{\pm \frac{\pi}{2\Delta}|\varepsilon - \mu|})$$

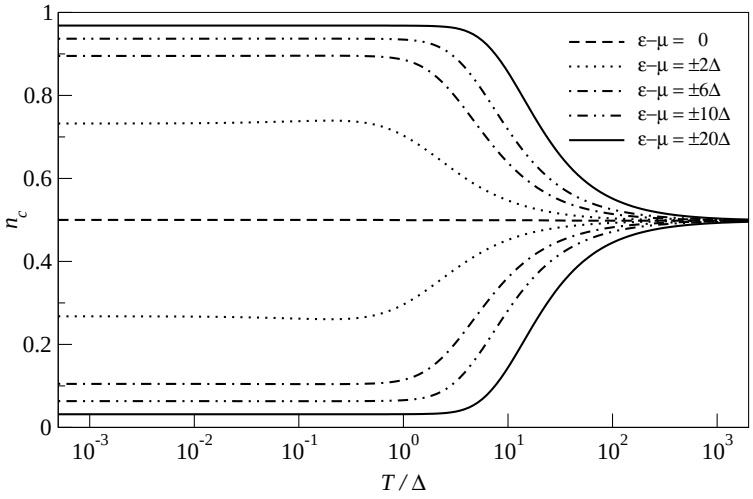

Figure 6. Charge content of the impurity site as a function of temperature for different values of $\varepsilon - \mu$. At high temperatures all curves start from $n_c = 1/2$ and flow, as the temperature is lowered to specific values $n_c^0\,(\varepsilon - \mu)$.

with $1 < a < 4$. For large $|\varepsilon - \mu|$ the two peaks are clearly separated and the *area*[1] under the Kondo peak is $k_B \ln\sqrt{2}$ while that under the Schottky peak is $k_B \ln 2$.

As mentioned earlier, the model was proposed as a description for the uranium ion physics of UBe_{13}. It is expected to describe the lattice above some coherence temperature. We provide in the inset of Fig. 2 the experimental data for the 5f-derived specific heat of the compound. It is obtained by subtracting from its total specific heat, the specific heat of the isostructural compound $ThBe_{13}$ containing no 5f electrons (10, 11). This way one is subtracting the phonon contribution as well as the electronic contribution from electrons in s, p and d shells (the procedure is quite involved and we refer the reader to the cited articles for full details). The sharp feature at $\sim 0.8K$ signals the superconducting transition of UBe_{13} and falls outside the range where this compound might be described by considering a single impurity model.

In order to be certain of having eliminated lattice effects it would be better to carry out the measurements on $U_{1-x}Th_xBe_{13}$. For $x > 0.1$ the compound has no longer a superconducting transition and the lattice coherence effects are largely suppressed. Further, there are several experimental

[1] Here by *area* we mean the following integral: $\int C_v\,(T)\;\; d\,(\ln T)$. In other words, the area as plotted, i.e. in a logarithmic scale.

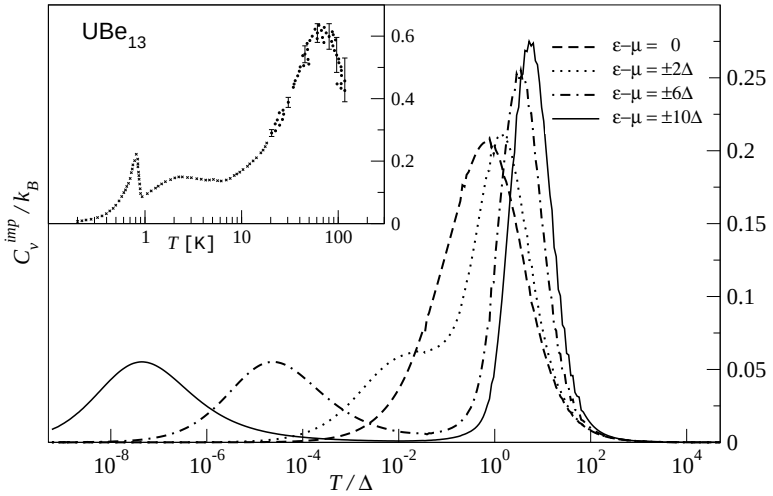

Figure 7. Main plot: impurity contribution to the specific heat as a function of temperature for different values of $\varepsilon - \mu$. As this parameter approaches zero the Kondo contribution (left) and the Schottky anomaly (right) collapse in a single peak. Inset: experimental data for the $5f$-derived specific heat of UBe_{13}.

indications that support the idea of an impurity model description of the thoriated compound for a wide range of temperatures (12).

Concentrating on the temperature range containing the Kondo and Schottky peaks we conclude that no values of ε and Δ of the 2-channel model yield a good fit. Further, the entropy obtained by integrating the weight under the experimental curve falls between $k_{\rm B} \ln 4$ and $k_{\rm B} \ln 6$. This suggests that a full description of the impurity may involve another high energy multiplet (possibly a Γ_4 triplet, cf. with the work of Koga and Cox (8)) close to the Γ_3 to yield the peak for the Schottky anomaly, with the Γ_6 doublet falling outside the range of measurements. The nature of the multiplet could be deduced from further specific heat measurements. For an n-plet degenerate with the Γ_3, one has an $SU(2) \otimes SU(n+2)$ Anderson model and the area under $C_{\rm v}^{\rm imp}/T$ is then given by $k_{\rm B} \ln[\frac{n+4}{2} \sec \frac{\pi}{n+4}]$, while if the n-plet is slightly split off the doublet, the area is given by $k_{\rm B} \ln[\frac{n+4}{\sqrt{2}}]$ (13). Also the scale of energy involved is then determined by crystal field splitting and corresponds to the scale observed. The split off non-magnetic triplet (i.e. $n = 3$ in the f^2 configuration seems, indeed, to be the most reasonable scenario for UBe_{13}. We are currently working in this direction.

Acknowledgements

We thank the organizers for the invitation to participate in the NATO Advanced Research Workshop on Concepts in Electron Correlation.

References

1. D. L. Cox, Phys. Rev. Lett. **59**, 1240 (1987).
2. A. P. Ramirez *et al.*, Phys. Rev. Lett. **73**, 3018 (1994).
3. F. G. Aliev *et al.*, Europhys. Lett. **32**, 765 (1995).
4. A. Schiller, F. B. Anders, and D. L. Cox, Phys. Rev. Lett. **81**, 3235 (1998).
5. D. L. A. Cox and A. Zawadowski, *Exotic Kondo Effects in Metals: Magnetic ions in a crystaline electric field and tunnelling centres* (Taylor & Francis, London UK, 1999).
6. D. L. Cox and A. E. Ruckenstein, Phys. Rev. Lett. **71**, 1613 (1993).
7. J. Kroha and P. Wölfle, Act. Phys. Pol. B **29**, 3781 (1998).
8. M. Koga and D. L. Cox, Phys. Rev. Lett. **82**, 2575 (1999).
9. C. J. Bolech and N. Andrei, Phys. Rev. Lett. **88**, 237206 (2002).
10. R. Felten *et al.*, Europhys. Lett. **2**, 323 (1986).
11. R. Felten, G. Weber, and H. Rietschel, J. Magn. Magn. Mat. **63 & 64**, 383 (1987).
12. F. G. Aliev, S. Viilar, and V. V. Moshchaikov, J. Phys. Cond. Matt. **8**, 9807 (1996).
13. A. Jerez, N. Andrei, and G. Zaránd, Phys. Rev. B **58**, 3814 (1998).